Proc. Natl. Acad. Sci. USA
Vol. 89, pp. 1214–1218, February 1992
Biophysics

Solid–liquid phase boundaries of lens protein solutions

(γ-crystallin/solubility/crystallization/phase transition)

CAROLYN R. BERLAND, GEORGE M. THURSTON*, MAMORU KONDO†, MICHAEL L. BROIDE‡, JAYANTI PANDE, OLUTAYO OGUN, AND GEORGE B. BENEDEK§

Department of Physics and Center for Materials Science and Engineering, Massachusetts Institute of Technology, Cambridge, MA 02139

Contributed by George B. Benedek, November 8, 1991

ABSTRACT **We report measurement of the solid–liquid phase boundary, or liquidus line, for aqueous solutions of three pure calf γ-crystallin proteins: γII, γIIIa, and γIIIb. We also studied the liquidus line for solutions of native γIV-crystallin calf lens protein, which consists of 85% γIVa/15% γIVb. In all four proteins the liquidus phase boundaries lie higher in temperature than the previously determined liquid–liquid coexistence curves. Thus, over the range of concentration and temperature for which liquid–liquid phase separation occurs, the coexistence of a protein crystal phase with a protein liquid solution phase is thermodynamically stable relative to the metastable separated liquid phases. The location of the liquidus lines clearly divides these four crystallin proteins into two groups: those in which liquidus lines flatten at temperatures >70°C: γIIIa and γIV, and those in which liquidus lines flatten at temperatures <50°C: γII and γIIIb. We have analyzed the form of the liquidus lines by using specific choices for the structures of the Gibbs free energy in solution and solid phases. By applying the thermodynamic conditions for equilibrium between the two phases to the resulting chemical potentials, we can estimate the temperature-dependent free energy change upon binding of protein and water into the solid phase.**

Maintenance of the lens proteins in a single homogenous fluid phase is an essential condition for transparency of the eye lens (1, 2). Consequently, we previously investigated the location of the coexistence curve (3–5) for liquid–liquid phase separation for four pure calf γ-crystallin protein solutions. In those studies, preliminary findings at a few points in the phase diagram suggested that the coexistence curve for solid–liquid phase equilibrium might be higher in temperature than the liquid–liquid coexistence curve (4, 5). We, therefore, undertook the present systematic investigation of the location of the solid–liquid coexistence curve for three pure lens crystallin proteins γII, γIIIa, and γIIIb, as well as for native γIV protein, which is a mixture of γIVa and γIVb in relative proportion of 85% to 15%, respectively, by number. We report here the measurement for each protein of the ascending limb of the solid–liquid coexistence curve. This limb is called the liquidus line; it is defined as the locus of points in the concentration (c) and temperature (T) plane that corresponds to equilibrium between protein crystals and an aqueous liquid solution of the same protein having concentration c. This locus can be designated by $T_L(c)$, or alternatively $c_L(T)$. At fixed temperature T, the concentration c_L is the solubility of the protein in aqueous solution. The descending limb of the solid–liquid coexistence curve is called the solidus line $c_s(T)$, and it is the locus of points showing the protein concentration in the solid phase for each temperature T. For $c_L(T) < c < c_s(T)$, the equilibrium state of the solution consists of a mixture of protein crystals of protein concentration $c_s(T)$ and aqueous liquid solution of protein concentration $c_L(T)$. In all our studies the solution conditions were maintained at pH 7.1 by using a 100 mM sodium phosphate buffer.

The solid–liquid coexistence curve for protein–water–salt solutions is of considerable interest for several reasons. (*i*) This coexistence curve describes the fundamental equilibrium solution conditions necessary to permit growth of protein crystals. Such crystals are essential for x-ray determination of the three-dimensional structures of proteins. (*ii*) The solid–liquid coexistence curve, along with the liquid–liquid coexistence curve, provides a quantitative measure of the structure of the underlying Gibbs free energy of the protein and water molecules in both liquid and solid phases. The case of the γ-crystallin calf lens proteins is particularly interesting because these proteins demonstrate vividly that relatively small changes in amino acid sequence can dramatically affect the location of the liquidus lines. The proteins studied are all monomeric, having 173–174 residues and a molecular mass of ≈21 kDa. Comparison of their amino acid sequences shows these proteins to be >70% homologous (6). Nevertheless, as we report below, slight differences in sequence among these proteins shift the location of the liquidus lines greatly.

MATERIALS AND METHODS

Measurement of Liquidus Lines. Liquidus lines were determined by two methods. (*i*) Changes in the size of protein crystals in contact with a solution of known concentration were directly visually detected by using a Nikon Optiphotopol microscope. Crystal melting was seen as the temperature of the crystal and solution was raised above the liquidus line. The observed melting temperature was an upper bound on the liquidus temperature. Conversely, as the temperature was lowered below the liquidus line, growth was observed when the rate of growth was at least 5 μm/hr. If growth was observed, this freezing temperature provided a lower bound on the liquidus temperature. Slides were prepared by placing ≈15 μl of solution of known concentration on a slide and then transferring a small number of crystals to the liquid drop by pipet. The drop was then covered with a cover slip sealed with silicone grease to prevent evaporation. The slide was placed on an Instec HS1 temperature-controlled hot stage (Boulder, CO), and its temperature was changed in small steps over a sufficient range to permit observation of either melting or growth. A video record of the process was maintained that allowed comparison of the shape and size of a crystal at two different temperatures. These comparisons

The publication costs of this article were defrayed in part by page charge payment. This article must therefore be hereby marked "*advertisement*" in accordance with 18 U.S.C. §1734 solely to indicate this fact.

*Present address: Oculon Corp., 26 Landsdowne St., Cambridge, MA 02139.
†Present address: Rigaku Corp., 3-9-12 Matsubara-Cho, Akishima-Shi, Tokyo 196, Japan.
‡Present address: Service de Physique de l'Etat Condensé, Centre d'Etudes de Saclay, F-91191 Gif-sur-Yvette Cedex, France.
§To whom reprint requests should be addressed.

permitted sensitive detection of the first signs of crystal growth or melting.

This method has three advantages. First, it uses very small amounts of protein. Second, the method is fairly rapid; a point on the liquidus can be determined in a few hours. Finally, by this means we can observe the kinetics of crystal growth and melting. The method is most accurate for crystals with rapid kinetics of growth and melting because then changes are readily apparent during observation. We took precautions to ensure accuracy in measuring the solution concentration. Because the samples are very small, crystal growth or melting could significantly perturb the initially measured concentration of the liquid drop. We minimized this effect by attempting to detect the earliest signs of growth or melting and adjusting the temperature to minimize changes in crystal volume. Also, the introduction of crystals to the slide, along with small amounts of the mother liquor, changed the initially measured concentration of the liquid drop. To mitigate this problem, the crystals were rinsed with protein solution of the desired concentration, and the smallest possible number of crystals was introduced into the solution on the slide. It was also necessary to control the rate of temperature sweep, so that the solution temperature always remained in equilibrium with that of the stage. (Equilibration times for a slide were measured by bonding a thermocouple to a test slide and comparing its reading to the measured stage temperature.) The liquidus lines for γIIIa-, γIIIb-, and γIV-crystallins were measured by using this method. The liquidus line for γII was measured by a second method described below.

In the second method, we monitored the concentration of a protein solution at fixed temperature in contact with protein crystals. The concentration of the solution either increased as some crystals dissolved or decreased as crystals grew until the solution–crystal system was in equilibrium. The system was determined to be in equilibrium when the measured concentration of the solution reached a constant value for a given temperature. This concentration–temperature pair is a point on the liquidus line. Temperature was fixed by means of a stirred water bath, and the system was sonicated periodically to ensure thorough mixing of all components. With this method very precise values for both concentration and temperature of the solution at the liquidus boundary can be obtained. This method has the disadvantage of being very slow. This method also becomes increasingly difficult to use for temperatures >35°C because evaporation of the protein solution is difficult to prevent. The liquidus line for γII-crystallin was measured by using this method, which has been described in greater detail by Kondo (7).

Protein Isolation and Purification. The γ-crystallins used were isolated from 1- to 6-week-old calf lenses, obtained by overnight express from Antech, Tyler, TX. The monomeric γ-crystallins were prepared from the soluble protein fraction by size-exclusion chromatography on Sephadex G-75 as described earlier (4). Native γ-crystallin so obtained was further fractionated into γI, γs, γII, γIII, and γIV by cation-exchange chromatography on Sulfopropyl Sephadex C-50, essentially according to Björk (8) and Thomson *et al.* (4). The γII fraction was further purified by using anion-exchange chromatography on DEAE-cellulose (7). Anion-exchange chromatography on DEAE-Sephadex was used to fractionate γIII into γIIIa and γIIIb as described in Broide *et al.* (3). Purity of the γIIIa and γIIIb fractions was at least 95%, based on chromatography and isoelectric focusing. All liquidus lines were determined with crystals prepared from freshly purified fractions.

The purified crystallin fractions were dialyzed exhaustively into 100 mM sodium phosphate buffer (ionic strength 240 mM, pH 7.1), which contained sodium azide (3 mM). These dialyzed solutions were then concentrated by ultrafiltration. Solutions were concentrated at temperatures below the liquidus line to avoid any risk of heat denaturation. It was necessary to take some precautions to obtain single-phase solutions. Protein solutions were filtered, and clean, dust-free glassware was used to minimize crystal nucleation sites. To obtain very concentrated samples ($c > 200$ mg/ml) liquid–liquid phase separation was induced by lowering the temperature of the sample to beneath the critical point, and the protein-rich lower phase was collected. All concentrations were determined by measuring the UV absorbance at 280 nm by using the extinction coefficients shown in Table 1. These coefficients of 0.1% by weight were determined gravimetrically as described in Broide *et al.* (3).

Table 1. Extinction coefficients and parameters used in analysis of liquidus lines

Protein	$E_{280}^{0.1\%,1\text{ cm}}$	T_c(K)[3]	w[9,10]	$\bar{\phi}^c$	κ	γ
γIIIa	2.33 ± 0.02	309.5		0.62	500	830
γIV	2.16 ± 0.13	311.0		0.62	500	820
γII	2.18 ± 0.07	278.4	0.65	0.57	628	850
γIIIb	2.11 ± 0.02	278.4	0.47	0.40	1316	870
γIVa			0.70	0.62	500	

In most cases the crystals used formed spontaneously from solutions at room temperature. Some crystals of γII were also prepared by concentrating a pure solution to very high concentrations (≈400 mg/ml) by rotary evaporation at room temperature (7). Under these conditions large crystals of γII formed on the walls of the evaporation flask.

RESULTS

In Fig. 1 we show the location of the liquidus lines in relation to the liquid–liquid coexistence curves for each protein studied. The upper curve in each case is the liquidus line; the lower line is a power-law fit to the coexistence curve as found by Broide *et al.* (3). In all cases the liquidus line is well above the coexistence curve. Liquid–liquid phase separation is actually metastable with respect to crystal formation. Therefore, an attempt to determine the coexistence curve by cloud point measurements may be obscured by crystal formation (4, 9). Fig. 2 shows the liquidus lines for γIIIa- and γIV-crystallins plotted on an expanded scale. These proteins denature at 65–70°C. Therefore, we were unable to extend our measurements of the liquidus line to temperatures greater than ≈60°C.

The liquidus lines of γIIIa- and γIV-crystallins are ≈30°C higher than those of γII- and γIIIb-crystallins. From this difference in location of the liquidus lines, we have divided the proteins into two groups: the high-melting-point protein group γIIIa and γIV and the low-melting-point protein group

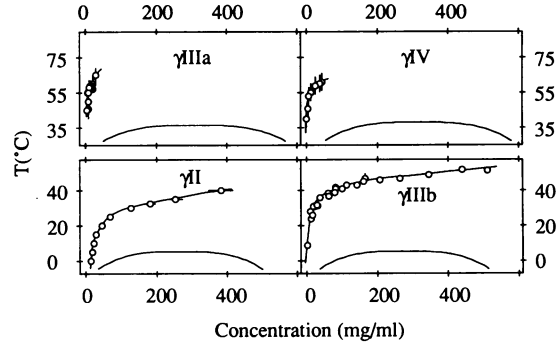

FIG. 1. Phase diagrams of each crystallin studied measured at pH 7.1 in 100 mM sodium phosphate buffer (ionic strength 240 mM). Upper curves are the liquidus boundaries; lower curves are power-law fits to the liquid–liquid coexistence boundary (3). Note that the upper two graphs are plotted over a higher range of temperatures than the lower two graphs. Temperature intervals are the same for all plots.

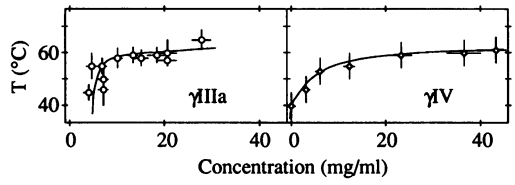

FIG. 2. Liquidus lines for γIIIa- and γIV-crystallins on an expanded concentration scale.

γII and γIIIb. The proteins have been divided into the same two groups based on their critical temperatures for binary liquid–liquid phase separation (3). The high-melting-point proteins are also the high-T_c proteins and have critical temperatures >35°C. The low-melting-point proteins are also the low-T_c proteins and have critical temperatures of ≈5°C. For each protein the separation between its critical point temperature and its melting temperature near the critical concentration is ≈30–40°C.

During our measurements we have obtained preliminary data on the kinetics of crystal melting and growth. The two high-melting-point crystallins have slow kinetics. Crystals of γIIIa are of approximately cubic form. They melt with rates of ≈0.1 μm/min. These crystals grow at rates of <0.02 μm/min. Crystal growth and melting rates for γIV are similar to those of γIIIa. The slow kinetics of these crystals means that only small changes in crystal size are seen during our 3- to 4-hr observation.

The low-melting-point proteins have faster kinetics than the high-melting-point proteins. Crystals of γII melt at rates of ≈0.4 μm/min. Data on the growth rates of γII crystals were not collected. Needle-shaped crystals of γIIIb melt along the crystal axis extremely rapidly with rates of 5 μm/min. They also grow rapidly at ≈1 μm/min. The rapid rate of melting and freezing in the γIIIb crystals meant that we could observe melting very easily during a 3- to 4-hr observation. Consequently we have obtained the liquidus line of γIIIb-crystallin with greater precision than the liquidus lines of γIIIa- and γIV-crystallins.

DISCUSSION

Location of the two branches of the solid–liquid coexistence curve—the liquidus line and the solidus line—can be obtained from the analytical forms of the Gibbs (or Helmholtz) free energies, which individually describe the solution phase and the solid crystal phase. We now present physically plausible choices for the form of the free energies in these two phases and use these to determine the physical information contained in our measurements of the liquidus lines.

Consider first the solution phase. This phase consists of N_p protein molecules each of volume Ω_p and N_w water molecules of volume Ω_w. The fixed total solution volume V is then $V = N_p\Omega_p + N_w\Omega_w$. Generally the Gibbs free energy G_s of the solution is a function of temperature T, pressure P, N_p, and N_w. It is convenient, however, to describe protein–water solutions in terms of the protein volume fraction $\phi = N_p\Omega_p/V$. We can then use a suitably normalized Gibbs free energy per particle $g_s(T, P, \phi)$, defined by the relation $g_s(T, P, \phi) = (\Omega_p/V)G_s(T, P, N_p, N_w)$. Because protein–water solutions can undergo binary–liquid phase separation, we choose a form of the free energy (10, 11) that predicts this separation in a qualitatively correct manner

$$g_s(T, P, \phi) = g_s^o(T, P, \phi) + kT\left\{\phi \ln\frac{\phi}{\gamma} - \frac{(\phi - 6\phi^2 + 4\phi^3)}{(1-\phi)^2}\right\} - c_2\phi^2. \quad [1]$$

Here $\gamma = (\Omega_p/\Omega_w)$, k is Boltzmann's constant and

$$g_s^o(T, P, \phi) = (\Omega_p/V)(N_p\mu_p^o + N_w\mu_w^o) = \phi\mu_p^o + \gamma(1-\phi)\mu_w^o. \quad [2]$$

g_s^o is the standard part of the normalized Gibbs free energy. μ_w^o is the change in G_s when a single water molecule is added to pure water. μ_p^o is taken here to be the change in G_s when a single protein molecule is added to a very dilute solution of protein molecules in pure water, apart from the contribution to this change due to the ideal entropy of mixing. Specifically, in the limit where $\delta N_p \to 0$ and $\gamma N_p << N_w$,

$$\mu_p^o = \frac{1}{\delta N_p}\left\{G_s(N_w, N_p + \delta N_p, P, T) - G_s(N_w, N_p, P, T) - kT\,\delta N_p \ln\left(\frac{N_p}{N_w + \gamma N_p}\right)\right\}.$$

It can readily be verified that Eqs. 1 and 2 are consistent with this definition. These standard potentials, by definition, depend only on T, P, and solution conditions (such as pH and ionic strength). The second term in Eq. 1 is the Carnahan–Starling form for the entropy of mixing of hard spheres (12). Such a form is expected to be appropriate for these globular proteins. The final term in Eq. 1 is a mean field quadratic form for the net interaction between protein molecules. Positive values of c_2 correspond to a net attraction between the protein molecules. Note that Eq. 1 is an approximation that is not intended to apply in the domain $\phi \to 1$. Indeed, in this domain, inspection of Eq. 1 shows an unphysical divergence in the model entropy.

Although all the equilibrium properties of the solution phase can be obtained directly from the free energy, it is more convenient to use the chemical potentials of the water and protein molecules $\mu_w = (\partial G_s/\partial N_w)_{T,P,N_p}$ and $\mu_p = (\partial G_s/\partial N_p)_{T,P,N_w}$. Using Eq. 1 we obtain

$$\mu_w = \mu_w^o - \frac{kT}{\gamma}\frac{(\phi + \phi^2 + \phi^3 - \phi^4)}{(1-\phi)^3} + \frac{c_2}{\gamma}\phi^2, \quad [3]$$

and

$$\mu_p = \mu_p^o + kT\left\{\ln\left(\frac{\phi}{\gamma}\right) + \frac{\phi(7 - 3\phi - \phi^2)}{(1-\phi)^2}\right\} + c_2\phi(\phi - 2). \quad [4]$$

In Eq. 1 the undetermined parameter c_2, which we assume is independent of temperature, can be fixed by using the thermodynamic stability conditions for binary–liquid phase separation. At the critical point (T_c, ϕ_c), $(\partial\mu_w/\partial\phi) = (\partial\mu_p/\partial\phi) = 0$; and $(\partial^2\mu_p/\partial\phi^2) = (\partial^2\mu_w/\partial\phi^2) = 0$. Use of these stability conditions in Eqs. 3 and 4 immediately fixes $c_2 = 10.6\,kT_c$ and predicts $\phi_c = 0.13$. This predicted value of ϕ_c is lower than the value of $\phi_c \cong 0.2$ measured by Broide *et al.* (3). This form of the free energy also predicts a liquid–liquid coexistence curve, which is narrower than the experimentally measured curve by a factor of ≈2.

We now turn to the thermodynamic specification of the crystal phase. Our description of the crystal phase must take into account the fact that protein crystals contain a large amount of water (in some cases >50% by weight) (13). In general then, the Helmholtz free energy of the crystal F_c (T, V^c, N_p^c, N_w^c) is a function of the temperature T; the total crystal volume V^c; and N_p^c and N_w^c, the number of protein molecules and water molecules, respectively, in the crystal. In principle, when the solid phase is in equilibrium with the solution phase at temperature T, the value of the four thermodynamic variables ϕ, N_p^c, N_w^c, and V^c can be determined by the following conditions. (*i*) The equality of pres-

sure in the two phases, (*ii*) the equality of the chemical potential of the protein in the solution phase with that in the crystal phase, (*iii*) the corresponding equality of the water chemical potential in the two phases, and (*iv*) the conservation of mass of protein and water in the two phases. We can proceed by making an alternative choice for the basic thermodynamic variables V^c, N_p^c, and N_w^c. We chose the new variables V^c, N_p^c, and κ. Here $\kappa \equiv N_w^c/N_p^c$ is the stoichiometric index. V^c is related to N_p^c and κ by $V^c = N_p^c(\Omega_p^c + \kappa\Omega_w^c)$, where Ω_p^c and Ω_w^c are the effective volumes occupied, respectively, by a protein and a water molecule in the crystal. We can then define a chemical potential of the crystal phase $\mu_c(T, n_c, \kappa)$ as

$$\mu_c(T, n_c, \kappa) = (\partial F_c/\partial N_p^c)_{T,V^c,\kappa}. \quad [5]$$

Here $n_c \equiv (N^c/V^c) \equiv N_p^c(1 + \kappa)/V^c$. Thus μ_c represents the change in Helmholtz free energy associated with adding a unit of one protein molecule and κ water molecules into the crystal phase. We now use the well-known Debye model for the Helmholtz free energy of the solid phase (14) to obtain the following expression for the chemical potential μ_c defined above:

$$\mu_c(T, n_c, \kappa) = E_B(T, n_c, \kappa) + 3kT \ln\left(2 \sinh \frac{\theta_D}{2T}\right). \quad [6]$$

Here $E_B(T, n_c, \kappa)$ is the binding energy in the crystal of one protein and κ water molecules, at temperature T, crystal density n_c and stoichiometric index κ. The second term in Eq. **6** is the contribution to the chemical potential from the lattice vibrations. Here θ_D is the Debye temperature that we shall regard as constant independent of temperature.

At each temperature T, the crystal phase has some definite value of the stoichiometric index κ. Thus, insofar as equilibrium under the transfer of matter between solid and solution phases is concerned we may visualize that the transfer of each protein molecule is accompanied by the transfer of κ water molecules. The corresponding condition on the chemical potentials that describes the equilibrium state of crystal and solution is

$$\mu_p(T, \phi) + \kappa\mu_w(T, \phi) = \mu_c(T, n_c, \kappa). \quad [7]$$

Eqs. **3** and **4** provide explicit expressions for $\mu_p(T, \phi)$ and $\mu_w(T, \phi)$ in the solution phase. Eq. **6** provides $\mu_c(T, n_c, \kappa)$. We may use the measured equilibrium values $\bar{\phi}$, $\bar{n}_c$, and $\bar{\kappa}$ of the thermodynamic variables at each temperature to gain insight into the free energy of the solid phase. To proceed in this direction we insert Eqs. **3**, **4**, and **6** into Eq. **7** and obtain an explicit formula for the quantity ε defined as

$$\varepsilon \equiv \frac{(\mu_p^o + \kappa\mu_w^o) - E_B(T, n_c, \kappa)}{kT_c}. \quad [8]$$

This important quantity measures the change in free energy associated with the transfer of one protein and κ water molecules between the solution phase and the crystal phase in terms of the energy scale kT_c. T_c is the critical temperature for binary liquid protein phase separation. From Eqs. **3–6** we find

$$\varepsilon = \left(\frac{T}{T_c}\right)\left\{3 \ln\left(2 \sinh \frac{\theta_D}{2T}\right) - \ln \frac{\phi}{\gamma} - \frac{\phi(7 - 3\phi - \phi^2)}{(1 - \phi)^2} + \frac{\kappa\phi(1 + \phi + \phi^2 - \phi^3)}{\gamma(1 - \phi)^3} + \frac{10.6T_c}{T}\left(2\phi - \phi^2 - \frac{\kappa}{\gamma}\phi^2\right)\right\}. \quad [9]$$

We may now insert into this equation the experimentally known values of $\bar{\phi}(T)$ along the liquidus line and $\bar{\kappa}(T)$ along the solidus line to determine $\varepsilon(T)$. The values of ε so deduced provide information on the crystal-binding energy $E_B(T, \bar{n}_c, \bar{\kappa})$. The values of $\bar{\phi}(T)$ are calculated from our measurements of the liquidus line by using the expression $\phi = \nabla c$ where ∇ is the partial specific volume of the protein (15) and c is the protein concentration in mg/cm^3. For γII-crystallin, $\nabla = 7.1 \times 10^{-4}$ cm^3/mg (5); we assume that the specific volume is approximately the same for the other γ-crystallins. In principle, the values of $\bar{\kappa}(T)$ and $\bar{n}_c(T)$ can be found from x-ray diffraction studies of the crystal in equilibrium with the solution at each temperature T. However, detailed measurements of x-ray structure have been made only at room temperature and only for the proteins γII, γIIIb, and γIVa (13, 16). In view of the weak dependence of ε on κ, we have assumed that the dependence of κ on T can be neglected over the range of T studied. We have also chosen to use the value of κ in γIVa crystals as an approximation for the corresponding values in γIIIa and γIV crystals. This choice seems plausible because γIV crystals probably are composed mostly of γIVa. γIIIa and γIV have similar liquidus lines.

In Table 1 we list the values of $\bar{\kappa}$, γ, and T_c for each protein for which we measured a liquidus line. κ is calculated from w, the measured protein weight fraction (13, 16), by using $\kappa = m_p(1 - w)/m_w w$, where m_w and m_p are, respectively, the molecular weight of the water and of the protein ($m_p \approx 21{,}000$ amu). We calculate $\gamma = m_p\bar{v}/(m_w/\rho_w)$, where ρ_w is the density of water in g/cm^3, using the exact molecular weights given by Björk (8) and White *et al.* (16) and $\bar{v}$ as given above. We also list in Table 1 the values of protein concentration in the crystal as both w, the protein weight fraction, and $\bar{\phi}^c$, the protein volume fraction. $\bar{\phi}^c$ is calculated from $\bar{\kappa}$ by using $\bar{\phi}^c = \gamma^c/(\gamma^c + \bar{\kappa})$. Here $\gamma^c = \Omega_p^c/\Omega_w^c$ is the ratio of the volume of the protein molecule to that of the water molecule in the crystal. We have assumed that the value of γ^c is approximately equal to γ, the value of this ratio in the solution phase. The listed values of $\bar{\phi}^c$ must be interpreted with caution because they are sensitive to the validity of this assumption. No direct measurements of θ_D for protein crystals have been made. However the softness of protein crystals suggests that θ_D is but a fraction of room temperature. Frauenfelder *et al.* (17) estimated the Debye temperature of an individual metmyoglobin molecule as between 160 and 200 K. In this work we have arbitrarily chosen $\theta_D = 100$ K for all crystals studied.

A plot of the calculated value of ε vs. T for each of the crystallins is shown in Fig. 3. Note that within experimental error ε is a positive-valued, linear function of T. The positive value of ε indicates that the free energy of the crystal phase is lower than the standard chemical potential for the protein and $\bar{\kappa}$ water molecules in the solution. The high-melting-point proteins have larger values of ε than the low-melting-point

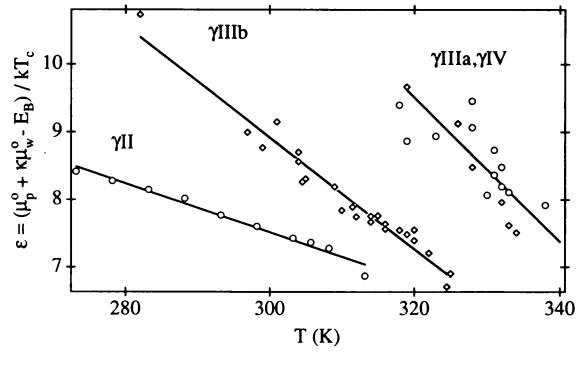

FIG. 3. Calculated value of ε as a function of temperature for each protein studied: γII-, γIIIa-, γIIIb-, and γIV-crystallins. Note that at a given temperature, the high-melting-point proteins have a higher value of ε than the low-melting-point proteins. (T_c for each protein is given in Table 1.)

proteins at a given temperature. The characteristic value of ε is $\approx 8\ kT_c$. However, the numerical values of ε are moderately sensitive to the choice of θ_D. ε remains a positive, linear function of T with nearly constant slope, as the value of θ_D varies between 50 and 200 K. But for a fixed T, the value of ε increases by $\approx 4\ kT$ as the choice for θ_D increases from 50 to 200 K. The value of ε is nearly independent of κ.

We can use the linear dependence of ε on T to check the consistency of our analysis of the binding energy. We fit the calculated values of $\varepsilon(T)$ for each protein to the linear function $\varepsilon(T) = \varepsilon_0 - \varepsilon_1 T$. When this expression for ε is inserted into Eq. 9, an implicit equation for $\overline{\phi}(T)$ results. The solution for $\overline{\phi}(T)$ is plotted for each protein in Fig. 4. The figure indicates that the theory presented above, when combined with a linear dependence of ε on temperature, provides a form of the liquidus line $\overline{\phi}(T)$ that is consistent with the data up to $\approx\phi = 0.2$. Above this volume fraction, the limitations of the present choice for the chemical potentials is seen by an increase of the theoretical prediction above the values found experimentally.

Summary and Conclusion. We have determined experimentally the location of the liquidus branch of the solid–liquid coexistence curve for aqueous solutions of three pure calf γ-crystallin proteins—γII, γIIIa, and γIIIb—and for native γIV, a mixture of γIVa- and γIVb-crystallins. We have theoretically analyzed these data with physically reasonable choices for the structure of the free energies of the solution and solid phases. The theory permits deduction of the free energy change (ε) associated with transferring one protein and the corresponding stoichiometric proportion of water molecules from the solution phase into the solid phase at each temperature for each protein studied. The magnitude of this energy change ε lies in the range 7–10 kT_c and decreases linearly with the temperature. In view of the importance of protein crystals for molecular biology, it is interesting to observe that systematic quantitative studies of the solid–liquid phase boundaries and the kinetics of crystal growth have been undertaken only relatively recently by a few research groups. G. Feher and his coworkers (18, 19) have produced a pioneering theoretical and experimental analysis of the kinetic factors that control the growth of crystals and amorphous precipitates. The equilibrium phase boundaries have more recently been studied in the cases of lysozyme (20–22), concanavalin A (23), and canavalin (24). The phase boundary between a solution phase and a polymerized gel phase of deoxyhemoglobin S has also been studied, and the enthalpy change accompanying this phase transition has been estimated (25–27). An important purpose of the present communication has been to bring to this subject insights from colloid physical chemistry and solid-state physics to formulate simple, physically sound models for the chemical potentials of protein and water in both solution and solid crystal phases. This investigation shows that such simple models can be used to understand quantitatively the experimentally observed form of the liquidus (or solubility) line over a very wide concentration range for the lens γ-crystallin proteins.

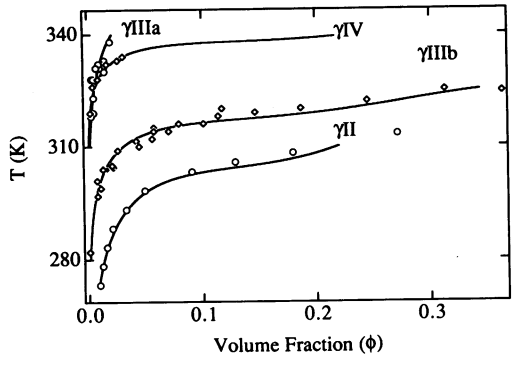

FIG. 4. Comparison of theoretically calculated liquidus lines (solid lines) with measured points (markers) for each of the proteins studied.

We thank Professor Felix Villars for a very helpful discussion on the thermodynamics of freezing. In particular, he pointed out the important Eq. 7. Professor Daniel Blankschtein first obtained Eqs. 3 and 4 for the chemical potential of protein and water in the solution phase. We thank Wasiq Bokhari for helping us collect the data on γIIIb-crystallin. We give special thanks to Mehmet Toner for helping us to develop the microscope-based technique used. We are grateful to Ajay Pande for measuring the extinction coefficients used. We also thank James Melhuish for technical assistance. Doo Soo Chung carefully read the manuscript. C.B. gratefully acknowledges support from the National Science Foundation Graduate Fellowship program. This work was supported by grants from the National Eye Institute of the National Institutes of Health (R01 EY05127) and the National Science Foundation (DMR 87-19217).

1. Delaye, M. & Tardieu, A. (1983) *Nature (London)* **302,** 415–417.
2. Benedek, G. B., Clark, J. I., Serrallach, E. N., Young, C. Y., Mengel, L., Sauke, A. & Benedek, K. (1979) *Philos. Trans. R. Soc. London.* **293,** 329–340.
3. Broide, M. L., Berland, C. R., Pande, J., Ogun, O. O. & Benedek, G. B. (1991) *Proc. Natl. Acad. Sci. USA* **88,** 5660–5664.
4. Thomson, J. A., Schurtenberger, P., Thurston, G. M. & Benedek, G. B. (1987) *Proc. Natl. Acad. Sci. USA* **84,** 7079–7983.
5. Schurtenberger, P., Chamberlin, R. A., Thurston, G. M., Thomson, J. A. & Benedek, G. B. (1989) *Phys. Rev. Lett.* **63,** 2064–2067.
6. Summers, L. J., Slingsby, C., Blundell, T. L., den Dunnen, J. T., Moormann, R. J. M. & Schoenmakers, J. G. G. (1986) *Exp. Eye Res.* **43,** 77–92.
7. Kondo, M. (1989) MS thesis (Massachusetts Institute of Technology, Cambridge).
8. Björk, I. (1964) *Exp. Eye Res.* **3,** 254–261.
9. Phillies, G. D. J. (1985) *Phys. Rev. Lett.* **55,** 1341.
10. Taratuta, V. G., Holschbach, A., Thurston, G. M., Blankschtein, D. & Benedek, G. B. (1990) *J. Phys. Chem.* **94,** 2140–2144.
11. Jansen, J. W., DeKruif, C. G. & Vrij, A. (1984) *Chem. Phys. Lett.* **107,** 450–453.
12. Carnahan, N. F. & Starling, K. E. (1969) *J. Chem. Phys.* **51,** 635–636.
13. Sergeev, Y. V., Chirgadze, Y. N., Mylvaganam, S. E., Driessen, H., Slingsby, C. & Blundell, T. L. (1988) *Proteins Struct. Func. Genet.* **4,** 137–147.
14. Wilson, A. H. (1957) *Thermodynamics and Statistical Mechanics* (Cambridge Univ. Press, Cambridge).
15. van Holde, K. E. (1985) *Physical Biochemistry* (Prentice-Hall, Englewood Cliffs, NJ), 2nd Ed.
16. White, H. E., Driessen, H. P. C., Slingsby, C., Moss, D. S. & Lindley, P. F. (1989) *J. Mol. Biol.* **207,** 217–235.
17. Frauenfelder, H., Hartmann, H., Karplus, M., Kuntz, I. D., Jr., Kuriyan, J., Parak, F., Petsko, G. A., Ringe, D., Tilton, R. F., Jr., Connolly, M. L. & Max, N. (1987) *Biochemistry* **26,** 254–261.
18. Kam, Z., Shore, H. B. & Feher, G. (1978) *J. Mol. Biol.* **123,** 539–555.
19. Feher, G. & Kam, Z. (1985) *Methods Enzymol.* **114,** 77–112.
20. Howard, S. B., Twigg, P. J., Baird, J. K. & Meehan, E. J. (1988) *J. Cryst. Growth* **90,** 94–104.
21. Ataka, M. & Asai, M. (1988) *J. Cryst. Growth* **90,** 86–93.
22. Pusey, M. L. & Gernert, K. (1988) *J. Cryst. Growth* **88,** 419–424.
23. Mikol, V. & Giege, R. (1989) *J. Cryst. Growth* **97,** 324–332.
24. DeMattei, R. C. & Feigelson, R. S. (1991) *J. Cryst. Growth* **110,** 34–40.
25. Prouty, M. S., Schechter, A. N. & Parsegian, V. A. (1985) *J. Mol. Biol.* **184,** 517–528.
26. Ross, P. D., Hofrichter, J. & Eaton, W. A. (1977) *J. Mol. Biol.* **115,** 111–134.
27. Eaton, W. A. & Hofrichter, J. (1990) *Adv. Protein Chem.* **40,** 63–279.